

Texture One Zero Dirac Neutrino Mass Matrix With Vanishing Determinant or Trace Condition

Madan Singh*

*Department of Physics, National Institute of Technology Kurukshetra,
Haryana, 136119, India.*

**singhmadan179@gmail.com*

May 8, 2018

Abstract

In the light of non-zero and relatively large value of reactor mixing angle (θ_{13}), we have performed a detailed analysis of texture one zero neutrino mass matrix M_ν in the scenario of vanishing determinant/trace conditions, assuming the Dirac nature of neutrinos. In both the scenarios, normal mass ordering is ruled out for all the six possibilities of M_ν , however for inverted mass ordering, only two are found to be viable with the current neutrino oscillation data at 3σ confidence level. Numerical and some approximate analytical results are presented.

1 Introduction

The Double Chooz, Daya Bay and RENO Collaborations [1–7] have finally established the non-zero and relatively large reactor mixing angle θ_{13} , therefore the number of precisely known neutrino oscillation parameters becomes five comprising two mass squared differences (δm^2 , Δm^2) and three neutrino mixing angles (θ_{12} , θ_{23} , θ_{13}). However, any general 3×3 neutrino mass matrix contains more parameters than can be measured in realistic experiments.

Several phenomenological schemes in particular, texture zeros [8–15] have been adopted in the literature in both flavor and non flavor basis, which not only allows to reduce the number of free parameters of M_ν , but also helps to establish some interesting relations between flavor mixing angles and fermion mass ratios [9]. Specifically, in the flavor basis wherein the charged lepton mass matrix is considered to be diagonal, a particular attention has been paid to explore the viability of texture zero mass matrices for Dirac [13, 14] as well as Majorana [8–12, 15] neutrinos with the experimental data. In Refs. [8–15], most of the texture zero analyses have been carried out assuming the Majorana nature of neutrinos, because various see-saw mechanisms for neutrino mass generation lead to light Majorana neutrinos.

However, considering the present ambiguity on neutrino mass, neutrinos could still be a Dirac particle. The highly-suppressed Yukawa couplings for Dirac neutrinos can naturally be achieved in the several models with extra spatial dimensions [16] or through radiative mechanisms [17] and also in supersymmetry models [18], supergravity models [19] of Dirac neutrino masses. Moreover, a common argument in favor of Majorana neutrinos is that the implied lepton number violation can be used to generate the baryon asymmetry of the universe via the leptogenesis mechanism [20]. However, similar argument can be made even for Dirac neutrinos [21,22].

Seeking the motivation for Dirac neutrinos from these theoretical grounds, Liu and Zhou [14] have carried out an analysis of texture zero mass matrices in the flavor basis, and found that all the six possibilities carrying one texture zero in the neutrino mass matrix are experimentally viable. This is not surprising as texture one zero makes available larger parametric space for viability with the data compared with texture two zero case. However, to impart predictability to texture one zero, additional constraints in the form of $\text{Det } M_\nu=0$ or $\text{Tr } M_\nu=0$ can be incorporated. The $\text{Det } M_\nu = 0$ [23] condition can be motivated on various theoretical grounds [24, 25]. The condition $\text{Det } M_\nu = 0$ is equivalent to assuming one of the neutrinos to be massless. This is realized, for instance, in the Affleck-Dine scenario for leptogenesis [26] which requires the lightest neutrino to be practically massless ($m \simeq 10^{-10}\text{eV}$) [27,28]. In Refs. [15,29], the implication for the same have been rigorously studied for texture one zero mass Majorana matrices. The motivation for $\text{Tr } M_\nu = 0$ condition, was first put forward in [30] applying a three neutrino framework that simultaneously explains the anomalies of solar and atmospheric neutrino oscillation experiments as well as the LSND experiment. In [31], X. G. He and A. Zee have investigated the CP conserving traceless M_ν for the more realistic case of explaining only the solar neutrino atmospheric and deficits. Further motivation of traceless mass matrices can be provided by models wherein M_ν is constructed through a commutator of two matrices, as it happens in models of radiative mass generation [32]. H. A. Alhendi et.al. [33] have incorporated the traceless condition with two 2×2 sub-matrices of Majorana mass matrix in the flavor basis and carried out a detailed numerical analysis at 3σ confidence level. Also the phenomenological implications of traceless M_ν on neutrino masses, CP violating phases and effective neutrino mass term is studied in Ref. [34], for both normal and inverted mass ordering and in case of CP conservation and violation.

Without loss of generality, we consider a neutrino mass matrix M_ν for Dirac neutrinos to be Hermitian by redefining the right-handed neutrino fields. As M_ν is Hermitian, three independent off-diagonal matrix elements are in general complex, while three independent diagonal ones are real. Following Ref. [14], the six possible texture one zero hermitian matrices are given in Table 1. The nomenclature is similar to texture one zero for Majorana neutrino except that here neutrino mass matrix is hermitian.

Textures P_2 and P_4 are related through permutation symmetry to P_3 and P_5 , respectively [14]. This corresponds to permutation of the 2-3 rows and 2-3 columns of M_ν . The corresponding permutation matrix is

P_1	P_2	P_3
$\begin{pmatrix} 0 & \Delta & \Delta \\ \Delta^* & \times & \Delta \\ \Delta^* & \Delta^* & \times \end{pmatrix}$	$\begin{pmatrix} \times & \Delta & \Delta \\ \Delta^* & 0 & \Delta \\ \Delta^* & \Delta^* & \times \end{pmatrix}$	$\begin{pmatrix} \times & \Delta & \Delta \\ \Delta^* & \times & \Delta \\ \Delta^* & \Delta^* & 0 \end{pmatrix}$
P_4	P_5	P_6
$\begin{pmatrix} \times & 0 & \Delta \\ 0 & \times & \Delta \\ \Delta^* & \Delta^* & \times \end{pmatrix}$	$\begin{pmatrix} \times & \Delta & 0 \\ \Delta^* & \times & \Delta \\ 0 & \Delta^* & \times \end{pmatrix}$	$\begin{pmatrix} \times & \Delta & \Delta \\ \Delta^* & \times & 0 \\ \Delta^* & 0 & \times \end{pmatrix}$

Table 1: Possible structures of neutrino mass matrices having texture one zero. where ‘ \times ’ stands for non-zero element and real matrix element and each ‘ Δ ’ for non-zero and complex entity.

$$P_{23} = \begin{pmatrix} 1 & 0 & 0 \\ 0 & 0 & 1 \\ 0 & 1 & 0 \end{pmatrix}. \quad (1)$$

As a result of permutation symmetry between different classes, one obtains the following relations among the oscillation parameters

$$\theta_{12}^X = \theta_{12}^Y, \quad \theta_{23}^X = 90^\circ - \theta_{23}^Y, \quad \theta_{13}^X = \theta_{13}^Y, \quad \delta^X = \delta^Y - 180^\circ, \quad (2)$$

where X and Y denote the textures related by 2-3 permutation.

In the present work, we attempt to investigate the phenomenological implications of texture one-zero neutrino mass matrices in the scenario of $\text{Det } M_\nu = 0$ or $\text{Tr } M_\nu = 0$ condition, assuming the Dirac nature of neutrinos. Earlier in [29], we have studied the implication of $\text{Det } M_\nu = 0$ on texture one zero mass matrices for Majorana neutrinos, and found that normal mass ordering is ruled out for all the six cases of texture one zero mass matrices, while only four cases P_2, P_3, P_4 and P_5 are found to be viable for inverted mass ordering at 3σ CL. However, in the present work, we find that only two cases P_2 and P_3 are able to survive the data for inverted mass ordering, while normal mass ordering remains ruled out for all the six cases at 3σ CL.

The rest of the paper is planned as follows: In section 2, we discuss the methodology used to reconstruct the neutrino mass matrix for Dirac neutrinos and hence obtain some useful phenomenological constraints on neutrino masses by imposing texture one zero and zero determinant (or trace) condition. In section 3, we present the numerical analysis using some analytical relations. In section 4, we summarize and conclude our work.

2 Methodology

In the flavor basis, where charged lepton mass matrix is assumed to be diagonal, the Dirac neutrino mass matrix M_ν , depending on three neutrino masses (m_1, m_2, m_3) and the flavor mixing matrix U is expressed as

$$M_\nu = U \begin{pmatrix} \lambda_1 & 0 & 0 \\ 0 & \lambda_2 & 0 \\ 0 & 0 & \lambda_3 \end{pmatrix} U^\dagger, \quad (3)$$

where $\lambda_1 = \eta.m_1, \lambda_2 = \kappa.m_2, \lambda_3 = m_3$ with $\eta.\kappa = \pm 1$. The three eigen values ($\lambda_1, \lambda_2, \lambda_3$) of a general 3×3 hermitian matrix are real, but not necessarily positive. For the present analysis, we adopt the following parameterization [11]

$$U = \begin{pmatrix} c_{12}c_{13} & s_{12}c_{13} & s_{13} \\ -c_{12}s_{23}s_{13} - s_{12}c_{23}e^{-i\delta} & -s_{12}s_{23}s_{13} + c_{12}c_{23}e^{-i\delta} & s_{23}c_{13} \\ -c_{12}c_{23}s_{13} + s_{12}s_{23}e^{-i\delta} & -s_{12}c_{23}s_{13} - c_{12}s_{23}e^{-i\delta} & c_{23}c_{13} \end{pmatrix}, \quad (4)$$

where $c_{ij} = \cos \theta_{ij}, s_{ij} = \sin \theta_{ij}$ ($i, j = 1, 2, 3$).

If one of the elements of M_ν is considered zero, i.e. $M_{lm} = 0$, it leads to following constraint equation

$$\eta.m_1 U_{l1} U_{m1}^* + \kappa.m_2 U_{l2} U_{m2}^* + m_3 U_{l3} U_{m3}^* = 0, \quad (5)$$

where l, m run over e, μ and τ . The solar and atmospheric mass squared differences ($\delta m^2, \Delta m^2$), where δm^2 corresponds to solar mass squared difference and Δm^2 corresponds to atmospheric mass squared difference, can be defined as

$$\delta m^2 = (m_2^2 - m_1^2), \quad (6)$$

$$\Delta m^2 = |m_3^2 - m_2^2|, \quad (7)$$

then the ratio of two mass-squared differences is given by

$$R_\nu = \frac{\delta m^2}{|\Delta m^2|}. \quad (8)$$

The Jarlskog rephrasing parameter J_{CP} , which measures the CP violation, is defined as

$$Im[K_{ij}^{lm}] = J_{CP} \sum_n \epsilon_{lmn} \sum_k \epsilon_{ijk}, \quad (9)$$

where $K_{ij}^{lm} = U_{li} U_{lj}^* U_{mi}^* U_{mj}$. The ϵ_{lmn} and ϵ_{ijk} denote the Levi-Civita symbols.

Noting that $\text{Det } M_\nu = 0$ if and only if $\text{Det } M^{diag} = 0$, where $M^{diag} = (\lambda_1, \lambda_2, \lambda_3)$, therefore $\text{Det } M_\nu = 0$ implies that one of the eigen values has to be zero. For the normal mass ordering (NO), $m_1 = 0$ and for inverted ordering (IO), $m_3 = 0$. The $\text{Tr } M_\nu = 0$ condition implies $\eta.m_1 + \kappa.m_2 + m_3 = 0$. In the following subsections, we shall study the implication of these conditions on one zero texture, separately.

2.1 $M_{lm} = 0$ with $\text{Det } M_\nu = 0$

First of all, we discuss the case of normal mass ordering (NO), which implies $m_1 = 0$. From Eq. (5), one can obtain the following constraint equation and hence deduce the neutrino mass ratio term $\frac{m_2}{m_3}$ as

$$\kappa \cdot m_2 U_{l2} U_{m2}^* + m_3 U_{l3} U_{m3}^* = 0, \quad (10)$$

and

$$\frac{m_2}{m_3} = -\frac{1}{\kappa} \frac{U_{l3} U_{m3}^*}{U_{l2} U_{m2}^*}. \quad (11)$$

In case $l = m$ (e.g. the one-zero textures $P_{1,2,3}$), Eq. (10) leads to one constraint condition, but we obtain two constraint conditions for $l \neq m$ case (e.g. the one-zero textures $P_{4,5,6}$). In the former case, $\kappa = -1$ must hold since neutrino mass ratios are by definition real and non-negative and

$$\frac{m_2}{m_3} = -\frac{1}{\kappa} \frac{|U_{l3}|^2}{|U_{l2}|^2}. \quad (12)$$

In the latter case, we can get two constraint conditions by equating the real and imaginary parts of Eq. (10) to zero

$$\text{Re}[K_{32}^{lm}] = -\kappa \left(\frac{m_2}{m_3} \right) |U_{l2}|^2 |U_{m2}|^2, \quad (13)$$

and

$$-\kappa \frac{1}{\left(\frac{m_2}{m_3} \right)} \frac{1}{|U_{l2}|^2 |U_{m2}|^2} \text{Im}[K_{32}^{lm}] = 0, \quad (14)$$

where $K_{ij}^{lm} = U_{li} U_{lj}^* U_{mi}^* U_{mj}$. Using Eqs. (6) and (7), neutrino masses (m_1, m_2, m_3) can be expressed in terms of experimentally known mass squared differences ($\delta m^2, \Delta m^2$) as

$$m_1 = 0, \quad m_2 = \sqrt{\delta m^2}, \quad m_3 = \sqrt{\delta m^2 + \Delta m^2}. \quad (15)$$

Hence, we obtain

$$\frac{m_2}{m_3} = \sqrt{\frac{R_\nu}{1 + R_\nu}}. \quad (16)$$

Using Eqs. (11) and (16), we can express R_ν in terms of mixing angles ($\theta_{12}, \theta_{23}, \theta_{13}$) and Dirac CP-violating phase (δ) as

$$R_\nu = \left[\left(\frac{U_{l2} U_{m2}^*}{U_{l3} U_{m3}^*} \right)^2 - 1 \right]^{-1}. \quad (17)$$

In case of inverted mass ordering (IO), which implies $m_3 = 0$, one obtain the following constraint equation using Eq. (5), and hence deduce the neutrino mass ratio term $\frac{m_2}{m_1}$ as

$$\eta \cdot m_1 U_{l1} U_{m1}^* + \kappa \cdot m_2 U_{l2} U_{m2}^* = 0, \quad (18)$$

$$\frac{m_2}{m_1} = -\frac{\eta}{\kappa} \frac{U_{l1}U_{m1}^*}{U_{l2}U_{m2}^*}. \quad (19)$$

Since mass ratio term $\frac{m_2}{m_1}$ is by definition real and non-negative, therefore $\eta = \pm 1, \kappa = \mp 1$ must hold. Using Eq. (19), one can deduce a constraint equation in case of $l = m$ (e.g. the one-zero textures $P_{1,2,3}$) in terms of mass ratio $\frac{m_2}{m_1}$

$$\frac{m_2}{m_1} = -\frac{\eta}{\kappa} \frac{|U_{l1}|^2}{|U_{l2}|^2}. \quad (20)$$

For $l \neq m$, one can equate the real and imaginary parts of Eq. (18) to zero and hence obtain the two constraint equations

$$Re[K_{12}^{lm}] = -\frac{\eta}{\kappa} \left(\frac{m_2}{m_1}\right) |U_{l2}|^2 |U_{m2}|^2, \quad (21)$$

$$-\frac{\eta}{\kappa} \frac{1}{\left(\frac{m_2}{m_1}\right)} \frac{1}{|U_{l2}|^2 |U_{m2}|^2} Im[K_{12}^{lm}] = 0. \quad (22)$$

The neutrino mass spectrum is given as

$$m_1 = \sqrt{\Delta m^2 - \delta m^2}, \quad m_2 = \sqrt{\Delta m^2}, \quad m_3 = 0, \quad (23)$$

The non-zero and finite mass ratio $\frac{m_2}{m_1}$ can be related to R_ν as

$$\frac{m_2}{m_1} = \frac{1}{\sqrt{1 - R_\nu}}. \quad (24)$$

Using Eqs. (19) and (24), we can express R_ν in terms of mixing angles ($\theta_{12}, \theta_{23}, \theta_{13}$) and Dirac CP violating phase (δ) as

$$R_\nu = 1 - \left(\frac{U_{l2}U_{m2}^*}{U_{l1}U_{m1}^*}\right)^2. \quad (25)$$

The Jarlskog rephrasing invariant parameter J_{CP} , which measures the CP violation, is defined as

$$Im[K_{ij}^{lm}] = J_{CP} \sum_n \epsilon_{lmn} \sum_k \epsilon_{ijk}. \quad (26)$$

In case of $M_{lm}=0$ with $m_1 = 0$, where $l \neq m$, Eq. (14) leads to either $\frac{m_3}{m_2} = 0$ or

$\frac{1}{|U_{l2}|^2 |U_{m2}|^2} = 0$ or $Im[K_{32}^{lm}] = 0$. From these possibilities, $\frac{m_3}{m_2} = 0$ implies $m_3 = 0$. With the help of Eq. (5), we obtain, $m_1 = m_2 = m_3 = 0$, which is in contradiction with the solar neutrino oscillation data (i.e. $m_2 > m_1$) [35, 36]. Moreover, the elements of mixing matrix U are always non-zero and finite, so we are left with $Im[K_{32}^{lm}] = 0$, which implies $J_{CP} = 0$. Therefore, CP violation is only possible for

the textures $P_{1,2,3}$ with $m_1 = 0$, while $\delta = 0^0$ or 180^0 holds for remaining one-zero textures viz. $P_{4,5,6}$. Similarly, in case of $M_{lm}=0$ with $m_3 = 0$, where $l \neq m$, Eq. (22) leads to either $\frac{m_1}{m_2} = 0$ or $\frac{1}{|U_{l2}|^2|U_{m2}|^2} = 0$ or $Im[K_{12}^{lm}] = 0$. Here $\frac{m_1}{m_2} = 0$ implies $m_1 = 0$. Using Eq. (5), we find $m_1 = m_2 = m_3 = 0$, which again contradicts the inequality relation $\delta m^2 > 0$ or equivalently $m_2 > m_1$ as established by the solar neutrino experiments. Therefore, we have only $Im[K_{12}^{lm}] = 0$ which implies $J_{CP} = 0$. Hence CP violation holds only for textures $P_{1,2,3}$ with $m_3 = 0$, while $\delta = 0^0$ or 180^0 holds for remaining one-zero textures viz. $P_{4,5,6}$.

2.2 $M_{lm} = 0$ with $\text{Tr } M_\nu = 0$

The second basis independent condition is $\text{Tr } M_\nu = 0$. The zero trace implies the sum of three neutrino eigen values of M_ν must be zero

$$\eta.m_1 + \kappa.m_2 + m_3 = 0 \quad (27)$$

Using Eqs. (5) and (27), we obtain the following relations for neutrino mass ratios

$$\alpha \equiv \frac{m_1}{m_3} = \frac{1}{\eta} \frac{U_{l2}U_{m2}^* - U_{l3}U_{m3}^*}{U_{l1}U_{m1}^* - U_{l2}U_{m2}^*}, \quad (28)$$

$$\beta \equiv \frac{m_2}{m_3} = \frac{1}{\kappa} \frac{U_{l3}U_{m3}^* - U_{l1}U_{m1}^*}{U_{l1}U_{m1}^* - U_{l2}U_{m2}^*}. \quad (29)$$

Since both α and β are by definition real and non-negative, the imaginary parts of the quantities on the right-hand side of Eqs. (28) and (29) have to disappear. This requirement may lead us to the determination of the CP violating phase δ , as we shall show below.

For $M_{lm} = 0$, where $l \neq m$ (e.g. textures $P_{4,5,6}$), one can again show that CP violation is forbidden. Using Eqs. (5) and (27) again and subsequently equating the imaginary part to zero, we obtain the following constraint equation

$$(2\eta\alpha + \kappa\beta)Im(K_{12}^{lm}) = 0. \quad (30)$$

Eq. (30) implies either $(2\eta\alpha + \kappa\beta) = 0$ or $Im(K_{12}^{lm}) = 0$. On solving $(2\eta\alpha + \kappa\beta) = 0$ and Eq. (27) simultaneously, we obtain $m_3 = \eta.m_1$, which is not possible. Therefore, we are left with $Im(K_{12}^{lm}) = 0$, which implies $J_{CP} = 0$. Hence CP violation is only possible for the textures $P_{1,2,3}$ and $\delta = 0^0$ or 180^0 for rest of the one zero textures. Therefore, it is concluded here that in both the scenarios, namely $\text{Det } M_\nu = 0$ and $\text{Tr } M_\nu = 0$, textures with vanishing diagonal entry lead to CP violation, while textures with vanishing off diagonal entry lead to CP conservation.

The ratio of two mass-squared differences R_ν and neutrino mass spectrum (m_1, m_2, m_3) in terms of neutrino mass ratios α and β can be given as

$$R_\nu = \frac{\delta m^2}{|\Delta m^2|} = \frac{(\beta^2 - \alpha^2)}{|1 - \beta^2|}, \quad (31)$$

Parameter	Best Fit	3σ
$\delta m^2 [10^{-5} eV^2]$	7.50	7.03 - 8.09
$ \Delta m_{31}^2 [10^{-3} eV^2]$ (NO)	2.52	2.407 - 2.643
$ \Delta m_{31}^2 [10^{-3} eV^2]$ (IO)	2.52	2.39 - 2.63
θ_{12}	33.56°	$31.3^\circ - 35.99^\circ$
θ_{23} (NO)	41.6°	$38.4^\circ - 52.8^\circ$
θ_{23} (IO)	50.0°	$38.8^\circ - 53.1^\circ$
θ_{13} (NO)	8.46°	$7.99^\circ - 8.90^\circ$
θ_{13} (IO)	8.49°	$8.03^\circ - 8.93^\circ$
δ (NO)	261°	$0^\circ - 360^\circ$
δ (IO)	277°	$145^\circ - 391^\circ$

Table 2: Current neutrino oscillation parameters from global fits at 3σ confidence level(CL) [37]. NO (IO) refers to normal (inverted) neutrino mass ordering.

$$m_3 = \sqrt{\frac{\delta m^2}{\beta^2 - \alpha^2}}, \quad m_2 = m_3 \beta, \quad m_1 = m_3 \alpha. \quad (32)$$

It must be noted that Eqs.(17), (25), (31) provide a very useful constraint to restrict the parameter space of neutrino oscillation parameters.

3 Numerical analysis

For the purpose of numerical calculations, we have used the 3σ values of the lepton mixing angles as well as neutrino mass square differences as listed in Table 2. To start with, we span the parameter space of input neutrino oscillation parameters $(\theta_{12}, \theta_{23}, \theta_{13}, \delta m^2, \Delta m^2)$ by choosing the randomly generated points of the order of 10^7 . Assuming the Dirac nature of neutrinos, we classify the six possible one-zero textures into two categories viz. CP violating textures (P_1, P_2, P_3) and CP conserving textures (P_4, P_5, P_6) , while for CP violating textures (P_1, P_2, P_3) , Dirac CP violating phase (δ) is allowed to vary between $[0^0, 360^0]$ at 3σ CL. For CP conserving textures (P_4, P_5, P_6) , only $\delta = 0^0$ or 180^0 are allowed. Using Eqs. (17), (25), (31), the parameter space of Dirac CP violating phase (δ) can be subsequently constrained. The present numerical analysis is divided into two parts : Firstly, we investigate the phenomenological consequences of zero determinant condition on one zero textures. The zero determinant condition implies either $m_1 = 0$ or $m_3 = 0$, corresponding to normal and inverted mass ordering, respectively. As a next step, we study the implication of zero trace for the same. In order to add more understanding to the phenomenological results, the approximate relation of mass ratios and R_ν have been taken into account up to the leading order term of $\sin\theta_{13}$. We emphasize here that the present numerical analysis is based on the exact formula not on approximations. The exact analytical relations for neutrino mass ratios for texture one zero mass matrices along with $\text{Det}M_\nu=0$ or $\text{Tr} M_\nu=0$ have been summarized in Table 3 4 5 .

$$(A) \quad M_{lm} = 0 \text{ with Det } M_\nu = 0$$

3.1 CP violating textures (P_1, P_2, P_3)

3.1.1 Texture P_1 with vanishing m_1 and m_3

For texture P_1 with $m_1 = 0$, one can obtain the full analytical expressions for mass ratio ($\frac{m_2}{m_3}$) and R_ν term from Eqs. (11) and (17)

$$\frac{m_2}{m_3} = -\frac{1}{\kappa} \frac{t_{13}^2}{s_{12}^2}, \quad (33)$$

$$R_\nu = \frac{t_{13}^4}{s_{12}^4 - t_{13}^4}, \quad (34)$$

where $\kappa = -1$ holds to ensure that $\frac{m_2}{m_3}$ is non-negative. Taking into account the 3σ experimental range of $(\theta_{12}, \theta_{13})$, we find that R_ν excludes the current experimental range. Similarly for $m_3=0$, we obtain $R_\nu = 1 - t_{12}^4 = 0.63 - 0.85$ from Eq. (25), which is again inconsistent with experimental range of R_ν . Hence, texture P_1 is ruled out with current experimental data for both $m_1 = 0$ and $m_3 = 0$ cases.

3.1.2 Texture P_2 with vanishing m_1 and m_3

For texture P_2 with $m_1 = 0$, we obtain the following relations in the leading order term of θ_{13}

$$\frac{m_2}{m_3} \approx -\frac{1}{\kappa} \frac{t_{23}^2}{c_{12}^2}, \quad (35)$$

$$R_\nu \approx \frac{t_{23}^4}{c_{12}^4 - t_{23}^4}, \quad (36)$$

where $\kappa = -1$ holds so as to get non-negative $\frac{m_2}{m_3}$. Using 3σ experimental range of mixing angles $(\theta_{12}, \theta_{23}, \theta_{13})$, R_ν turns out to be well above the current experimental range. Therefore, texture P_2 with $m_1 = 0$ is not consistent with the neutrino oscillation data at 3σ CL. On the contrary, texture P_2 with $m_3 = 0$ is found to be consistent with current experimental data at 3σ CL. The analytical expressions for mass ratios $\frac{m_2}{m_1}$ and R_ν (up to the leading s_{13} term) are presented below

$$\frac{m_2}{m_1} \approx -\frac{\eta}{\kappa} t_{12}^2 \left(1 + \frac{2c_\delta s_{13} t_{23}}{s_{12} c_{12}} \right), \quad (37)$$

$$R_\nu \approx 1 - \frac{1}{t_{12}^4} \left(1 - \frac{4c_\delta s_{13} t_{23}}{s_{12} c_{12}} \right), \quad (38)$$

where $c_\delta \equiv \cos\delta$. Here, $\eta = \pm 1, \kappa = \mp 1$ must hold so as to get non-negative $\frac{m_2}{m_1}$. Since $\delta m^2 > 0$ or equivalently $m_2 > m_1$, we have $\cos\delta > 0$ from Eq. (37), which

implies that Dirac CP violating phase (δ) lies in the first and fourth quadrant i.e. $\delta < 90^\circ$ and $\delta > 270^\circ$. From figure 1(a), it is evident that parameter space of Dirac CP phase lies in the range, $\delta \in [0^\circ, 56^\circ] \oplus [306^\circ, 360^\circ]$. The correlation plot for (m_1, m_2) indicates that there is strong linear correlation between m_1 and m_2 [figure 1(b)]. The parameter space of (J_{CP}, δ) shows that $J_{CP} \neq 0$, indicating the CP violation [figure 1(a)].

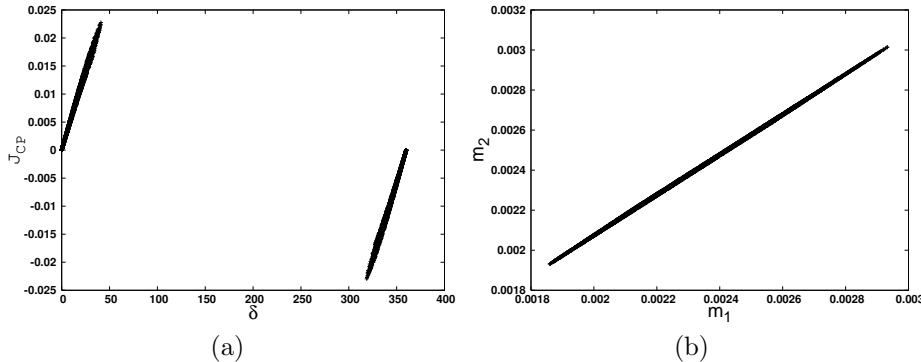


Figure 1: Correlation plots for texture P_2 with $m_3 = 0$. The masses m_1 and m_2 are measured in eV.

3.1.3 Texture P_3 with vanishing m_1 and m_3

As already pointed out in Section 2, the textures P_3 and P_2 are related due to 2-3 permutation symmetry. Therefore, texture P_3 with $m_1 = 0$ also remains inconsistent with current experimental data. Similar to the previous case for texture P_2 , texture P_3 with $m_3 = 0$ also favors the current neutrino oscillation data. With the help of Eqs. (19) and (25), we deduce some analytical expressions in the leading order of s_{13} term.

$$\frac{m_2}{m_1} \approx -\frac{\eta}{\kappa} t_{12}^2 \left(1 - \frac{2c_\delta s_{13}}{s_{12} c_{12} t_{23}} \right), \quad (39)$$

$$R_\nu \approx 1 - \frac{1}{t_{12}^4} \left(1 + \frac{4c_\delta s_{13}}{s_{12} c_{12} t_{23}} \right). \quad (40)$$

where $\eta = \pm 1, \kappa = \mp 1$. From Eq. (39), we have $\cos \delta < 0$ in view of the fact that $m_2 > m_1$, which implies that Dirac CP violating phase (δ) lies in the second and third quadrant i.e. $90^\circ < \delta < 270^\circ$. From figure 2(a), it is evident that parameter space of Dirac CP phase lies in the range, $\delta \in [130^\circ, 230^\circ]$. The allowed parameter space of δ can be further verified by using the relation, δ (for texture P_3) = δ (for texture P_2) $\pm 180^\circ$, resulting from the permutation symmetry. The correlation plot between m_1 and m_2 exhibits a linear correlation [figure 2(b)]. The CP-violation (implying $J_{CP} \neq 0$) in texture P_3 can be seen in figure 2(a) along with vanishing value of J_{CP} .

In figures 3(a) and 3(b), we have explicitly shown the permutation symmetry between textures P_2 and P_3 . Also, we can see that texture P_2 allows only upper octant of θ_{23} (i.e. $\theta_{23} > 45^\circ$), while texture P_3 allows only lower octant (i.e. $\theta_{23} < 45^\circ$). For higher values of reactor angle θ_{13} , θ_{23} is found to shift towards 45° . Figures 3(a) and 3(b) may appear to show slight deviation from the permutation symmetry relation:

$$\theta_{23}^{P_3} = 90^\circ - \theta_{23}^{P_2}. \quad (41)$$

However, this apparent deviation is just because the experimentally allowed 3σ range for θ_{23} is not symmetric around $\theta_{23} = 45^\circ$.

The $\text{NO}\nu\text{A}$ experiment has recently excluded the maximal-mixing value $\theta_{23} = 45^\circ$ at the 2.6σ confidence level [38], hence hints towards the non-maximality of θ_{23} . In Ref. [39–41] a slight preference for the upper octant (more pronounced in IO) has been indicated, although both octants are allowed at 2σ CL. The further robust measurement is needed to decide the octant of θ_{23} and hence the compatibility of above textures.

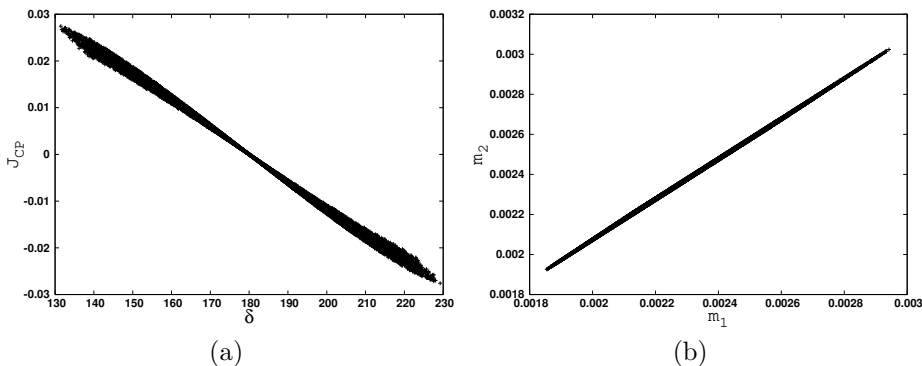


Figure 2: Correlation plots for textures P_3 with $m_3 = 0$. The masses m_1 and m_2 are measured in eV.

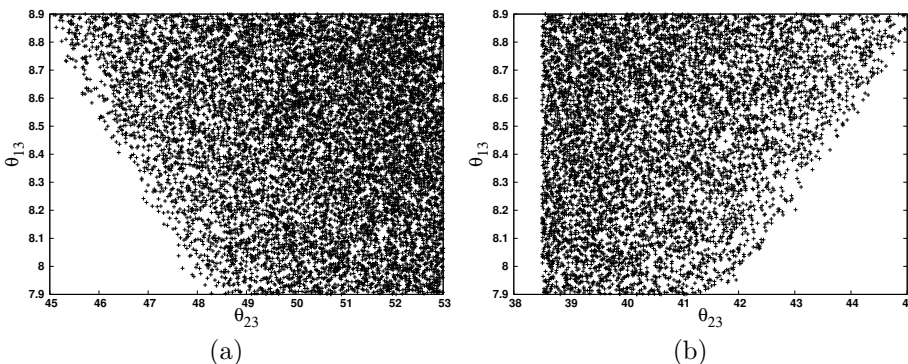


Figure 3: Correlation plots for textures (a) P_2 with $m_3 = 0$ and (b) P_3 with $m_3 = 0$, depicting the permutation symmetry.

3.2 CP conserving textures (P_4, P_5, P_6)

3.2.1 Texture P_4 with vanishing m_1 and m_3

With the help of Eq. (11), we obtain

$$\frac{m_2}{m_3} = -\frac{1}{\kappa} \frac{s_{13}s_{23}}{-s_{12}^2 s_{23} s_{13} \pm s_{12} c_{12} c_{23}}, \quad (42)$$

where $\kappa = -1$. The upper and lower signs correspond to $\delta = 0^\circ$ and 180° , respectively. Using Eqs. (11) and (17), one can deduce the mass ratio $\frac{m_2}{m_3}$ and R_ν terms

$$\frac{m_2}{m_3} \approx \frac{t_{23}s_{13}}{s_{12}c_{12}}, \quad (43)$$

$$R_\nu \approx \frac{t_{23}^2 s_{13}^2}{s_{12}^2 c_{12}^2}, \quad (44)$$

where s_{13} is expanded in leading order approximation. From above equation, it is clear that $R_\nu \propto s_{13}^2$, depends strongly on reactor mixing angle θ_{13} . The latest mixing data (at 3σ CL) leads to rather large R_ν , lying in the range $[0.05, 0.5]$ and hence excluded by current experimental range of R_ν .

On the other hand, for $m_3 = 0$, we obtain the following relations (in the leading order of s_{13} term) from Eqs. (19) and (25),

$$\frac{m_2}{m_1} \approx -\frac{\kappa}{\eta} \left(1 \pm \frac{t_{23}s_{13}}{s_{12}c_{12}} \right), \quad (45)$$

where $\eta \cdot \kappa = -1$ must hold. The upper and lower signs refer to the cases of $\delta = 0^\circ$ and 180° , respectively. From Eq. (45), $\delta = 180^\circ$ is disallowed since it leads to $m_2 < m_1$. Hence, for $\delta = 0^\circ$, we obtain

$$R_\nu \approx \frac{2t_{23}s_{13}}{s_{12}c_{12}}. \quad (46)$$

Using 3σ range of mixing angles, we obtain $0.467 \leq R_\nu \leq 0.963$, which is again in conflict with the experimental range of R_ν . Therefore, texture P_4 is not consistent with the neutrino oscillation data at 3σ CL, nor is the texture P_5 due to permutation symmetry.

3.2.2 Texture P_6 with vanishing m_1 and m_3

As already discussed in Section 3, there is no CP violation in this case. Therefore, only $\delta = 0^\circ$ or 180° is allowed. For texture P_6 with $m_1 = 0$, we can obtain the full analytical expression for mass ratio $\left(\frac{m_2}{m_3}\right)$ using Eq. (11)

$$\frac{m_2}{m_3} = -\frac{1}{\kappa} \frac{s_{23}c_{23}c_{13}^2}{(s_{12}^2 s_{13}^2 - c_{12}^2)c_{23}s_{23} + s_{12}c_{12}s_{13}(\pm s_{23}^2 \mp c_{23}^2)}, \quad (47)$$

where $\kappa = -1$ holds so as to get the non-negative mass ratio term $\frac{m_2}{m_3}$. The upper and lower signs correspond to $\delta = 0^\circ$ and 180° , respectively. In the leading order approximation of s_{13} , one can deduce the mass ratio $\left(\frac{m_2}{m_3}\right)$ as

$$\frac{m_2}{m_3} \approx \frac{1}{\kappa} \cdot \frac{1}{c_{12}^2}, \quad (48)$$

where $\kappa = 1$. From above equation, we find that $m_2 > m_3$, which is not possible in case of normal mass ordering ($m_1 = 0, m_2 < m_3$). Similarly, it is found that texture P_6 with $m_3 = 0$ also remains incompatible with current neutrino oscillation data [34]. With the help of Eq. (19), one can derive the full analytical expression for $\frac{m_2}{m_1}$

$$\frac{m_2}{m_1} = -\frac{\eta}{\kappa} \frac{s_{23}c_{23}(c_{12}^2s_{13}^2 - s_{12}^2) + s_{12}c_{12}s_{13}(\pm c_{23}^2 \mp s_{23}^2)}{s_{23}c_{23}(s_{12}^2s_{13}^2 - c_{12}^2) + s_{12}s_{13}c_{12}(\pm s_{23}^2 \mp c_{23}^2)}, \quad (49)$$

where $\eta \cdot \kappa = -1$. The upper and lower signs in the above expression refer to the cases $\delta = 0^\circ$ and 180° , respectively. In the leading order approximation of s_{13} , we deduce the mass ratio $\left(\frac{m_2}{m_1}\right)$ and R_ν as

$$\frac{m_2}{m_1} \approx t_{12}^2 \left(1 \mp \frac{2s_{13}}{t_{2(23)}s_{12}c_{12}} \right), \quad (50)$$

$$R_\nu \approx 1 - \frac{1}{t_{12}^4} \left(1 \pm \frac{4s_{13}}{t_{2(23)}s_{12}c_{12}} \right). \quad (51)$$

From the above equation, we find that $m_2 < m_1$ for both $\delta = 0^\circ$ and 180° , which contradicts the solar neutrino oscillation data. Therefore, texture P_6 with $m_3 = 0$ is ruled out with latest experimental data.

For sake of completion, we have provided the hermitian mass matrices for two allowed cases P_2 and P_3 of texture one zero with $\text{Det } M_\nu = 0$ condition.

$$M_\nu^{P_2} = \begin{pmatrix} a_{11} & a_{12} & a_{13} \\ a_{21} & a_{22} & a_{23} \\ a_{31} & a_{32} & a_{33} \end{pmatrix},$$

where

$$\begin{aligned} a_{11} &= 0.0104 - 0.0211, \\ a_{12} &= ((-0.0402) - (-0.0167)) + i((-0.0252) - 0.0250), \\ a_{13} &= (0.0183 - 0.0374) + i((-0.0314) - 0.0317), \\ a_{21} &= ((-0.0402) - (-0.0167)) - i((-0.0250) - 0.0250), \\ a_{22} &= 0.0, \\ a_{23} &= (0.00460 - 0.00907) + i((-0.00700) - 0.00682), \\ a_{31} &= (0.0183 - 0.0374) - i((-0.0314) - 0.0317), \\ a_{32} &= (0.00460 - 0.00907) - i((-0.00700) - 0.00682), \\ a_{33} &= (-0.0219) - (-0.0110), \end{aligned}$$

and

$$M_\nu^{P_3} = \begin{pmatrix} b_{11} & b_{12} & b_{13} \\ b_{21} & b_{22} & b_{23} \\ b_{31} & b_{32} & b_{33} \end{pmatrix},$$

where

$$\begin{aligned} b_{11} &= 0.0102 - 0.0194, \\ b_{12} &= (0.0199 - 0.0364) + i(-0.0288 - 0.0297), \\ b_{13} &= ((-0.0405) - (-0.0192)) + i((-0.0247) - 0.0236), \\ b_{21} &= (0.0199 - 0.0364) - i((-0.0288) - 0.0297), \\ b_{22} &= (-0.0201) - (-0.0111), \\ b_{23} &= (0.00492 - 0.00907) + i(-0.00640 - 0.00660), \\ b_{31} &= ((-0.0405) - (-0.0192)) - i((-0.0246) - 0.0236), \\ b_{32} &= (0.00492 - 0.00907) - i((-0.00640) - 0.00660), \\ b_{33} &= 0.0. \end{aligned}$$

$$(B) \quad M_{lm} = 0 \text{ with } \text{Tr } M_\nu = 0$$

After having discussed the texture one zero with $\text{Det } M_\nu=0$, we discuss the texture one zero with $\text{Tr } M_\nu=0$. It is found from our analysis that normal mass ordering is ruled out for all the six of neutrino mass matrix M_ν , while two of them (i.e. P_2 and P_3) in the case of inverted mass ordering are found to be compatible with experimental data at 3σ level. The survived textures are phenomenologically related to each other due to 2-3 permutation symmetry. From the analysis, we find that in case of $M_{lm} = 0$ with $\text{Tr } M_\nu = 0$, where $l = m$, only $\eta = +1$ and $\kappa = -1$ possibility holds in case of textures P_2 and P_3 as given in Table 6. Also, the exact analytical expressions for mass ratios (α, β) have been provided in Table 5. With the help of some approximate analytical relations of neutrino mass ratios, we have checked the viability of all the six with $\text{Tr } M_\nu=0$ condition.

3.3 CP violating textures (P_1, P_2, P_3)

3.3.1 Texture P_1 with $\text{Tr } M_\nu = 0$

Using Eqs. (28) and (29) and retaining only the leading order term of θ_{13} , we obtain following analytical relations

$$\alpha \equiv \frac{m_1}{m_3} \approx \frac{1}{\eta} \sec 2\theta_{12} s_{12}^2, \quad (52)$$

$$\beta \equiv \frac{m_2}{m_3} \approx -\frac{1}{\kappa} \sec 2\theta_{12} c_{12}^2, \quad (53)$$

where $\eta = +1$, $\kappa = -1$ so that α, β remain real and positive. Using Eqs. (52) and (53), we obtain $R_\nu \approx \beta^2 - \alpha^2 \approx \sec 2\theta_{12}$ for normal mass ordering. Using

3σ experimental range of oscillation parameter, we find, $2.23 \leq R_\nu \leq 4.02$, which excludes the experimental range of R_ν and for inverted mass ordering, we have

$$R_\nu \approx \frac{\sec 2\theta_{12}}{\sec^2 2\theta_{12} c_{12}^4 - 1}, \quad (54)$$

which is again inconsistent with current experimental data as $R_\nu > 0.75$. Therefore, texture P_1 with $\text{Tr } M_\nu = 0$ is ruled out according to latest neutrino oscillation data at 3σ CL.

3.3.2 Texture P_2 with $\text{Tr } M_\nu = 0$

Using Eqs. (28) and (29), we obtain the following analytical relations in the leading order approximation of θ_{13}

$$\alpha \equiv \frac{m_1}{m_3} \approx -\frac{1}{\eta} \sec 2\theta_{12} (c_{12}^2 - t_{23}^2), \quad (55)$$

$$\beta \equiv \frac{m_2}{m_3} \approx \frac{1}{\kappa} \sec 2\theta_{12} (s_{12}^2 - t_{23}^2). \quad (56)$$

Here, $\eta = +1, \kappa = -1$ must hold so as to get non-negative mass ratios $\frac{m_1}{m_3}$ and $\frac{m_2}{m_3}$. From figure 4(a), it is evident that parameter space of Dirac CP violating phase lies in the range, $\delta \in [0^0, 56^0] \oplus [306^0, 360^0]$. The parameter space of (J_{CP}, δ) shows that $J_{CP} \neq 0$, implying CP violation [figure 4(a)]. In figure 4(b, c), it is shown that only inverted mass ordering ($m_3 \ll m_1 < m_2$) is allowed for this texture, while normal mass ordering is ruled out.

3.3.3 Texture P_3 with $\text{Tr } M_\nu = 0$

Since texture P_3 is related to texture P_2 via permutation symmetry as mentioned earlier, the phenomenological implications for texture P_3 can be obtained from texture P_2 . With the help of Eqs. (28) and (29), we deduce some useful analytical relations in the leading order term of s_{13} term.

$$\alpha \equiv \frac{m_1}{m_3} \approx -\frac{1}{\eta} \sec 2\theta_{12} \left(c_{12}^2 - \frac{1}{t_{23}^2} \right), \quad (57)$$

$$\beta \equiv \frac{m_2}{m_3} \approx \frac{1}{\kappa} \sec 2\theta_{12} \left(s_{12}^2 - \frac{1}{t_{23}^2} \right). \quad (58)$$

Here, $\eta = +1, \kappa = -1$ must hold in order to obtain non-negative $\frac{m_1}{m_3}$ and $\frac{m_2}{m_3}$. From figure 4(a), it is evident that parameter space of Dirac CP phase lies in the range, $\delta \in [128.5^0, 231.5^0]$. The correlation plots for neutrino masses (m_1, m_2, m_3) indicates that only inverted mass ordering is allowed [figures 5 (b, c)]. In figure 5 (b), there exist a strong linear correlation between neutrino masses m_1 and m_2 . The parameter space of (J_{CP}, δ) indicates $J_{CP} \neq 0$, implying that texture P_3 exhibits

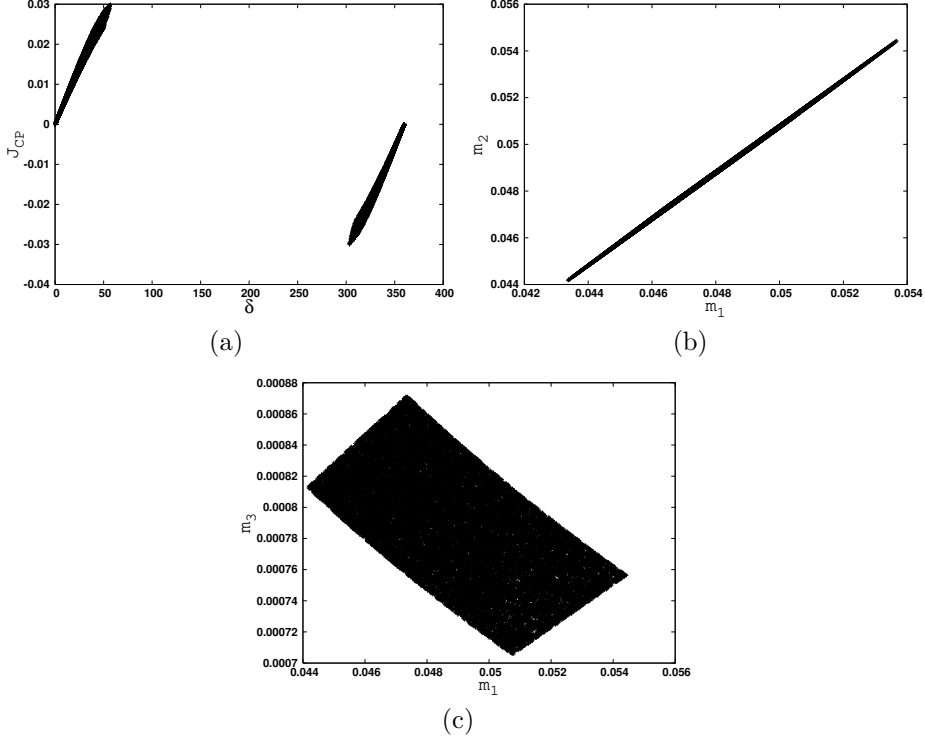


Figure 4: Correlation plots for P_2 with $\text{Tr } M_\nu = 0$. The neutrino masses $m_{1,2,3}$ are measured in eV.

CP violation [figure 5(a)]. In figures.6(a) and 6(b), we have provided the correlation plots between θ_{23} and θ_{13} for textures P_2 and P_3 , respectively. Unlike $\text{Det } M_\nu = 0$ case, textures P_2 and P_3 with $\text{Tr } M_\nu = 0$ prefer both the octant of θ_{23} . Again, permutation symmetry between P_2 and P_3 is clearly visible in figure 6(a, b).

3.4 CP conserving textures (P_4, P_5, P_6)

3.4.1 Texture P_4 with $\text{Tr } M_\nu = 0$

Using Eqs. (28) and (29), we obtain the following analytical expressions in leading order of s_{13} term

$$\alpha \equiv \frac{m_1}{m_3} \approx -\frac{1}{\eta} 0.5, \quad (59)$$

$$\beta \equiv \frac{m_2}{m_3} \approx -\frac{1}{\kappa} 0.5. \quad (60)$$

Since $R_\nu=0$ in the leading order approximation of s_{13} , we have to work at next to leading order of θ_{13}

$$\alpha \equiv \frac{m_1}{m_3} \approx -\frac{1}{\eta} \frac{1}{2} \left(1 \mp \frac{3}{2} \frac{s_{23}s_{13}}{c_{12}s_{12}c_{23}} \right) + O(s_{13}^2), \quad (61)$$

$$\beta \equiv \frac{m_2}{m_3} \approx -\frac{1}{\kappa} \frac{1}{2} \left(1 \pm \frac{3}{2} \frac{s_{23}s_{13}}{c_{12}s_{12}c_{23}} \right) + O(s_{13}^2). \quad (62)$$

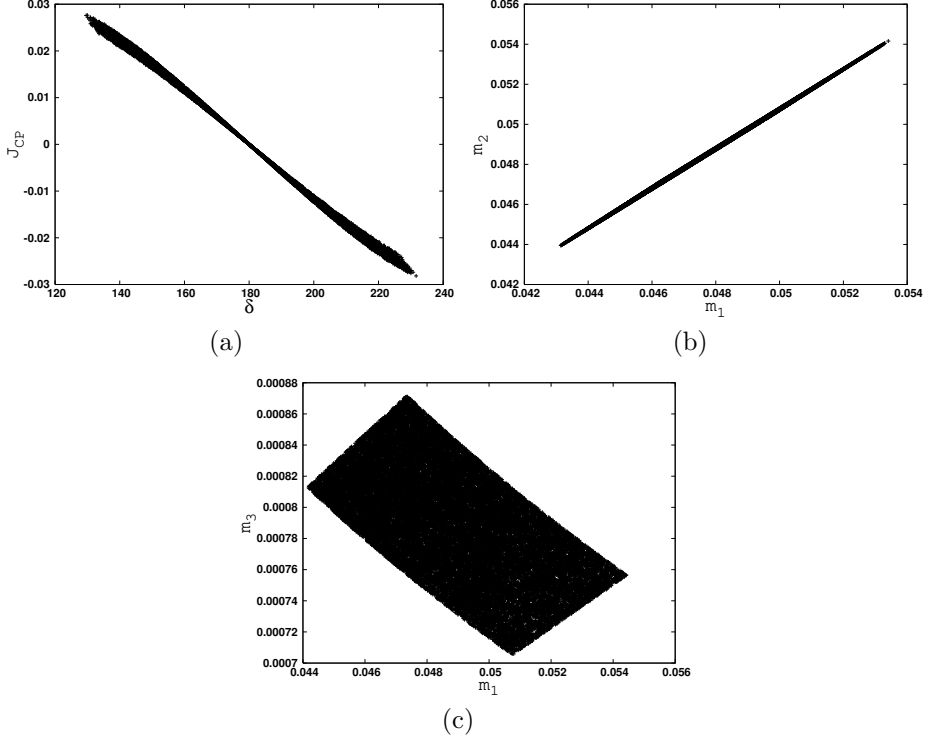


Figure 5: Correlation plots for P_3 with $\text{Tr } M_\nu = 0$. The neutrino masses $m_{1,2,3}$ are measured in eV.

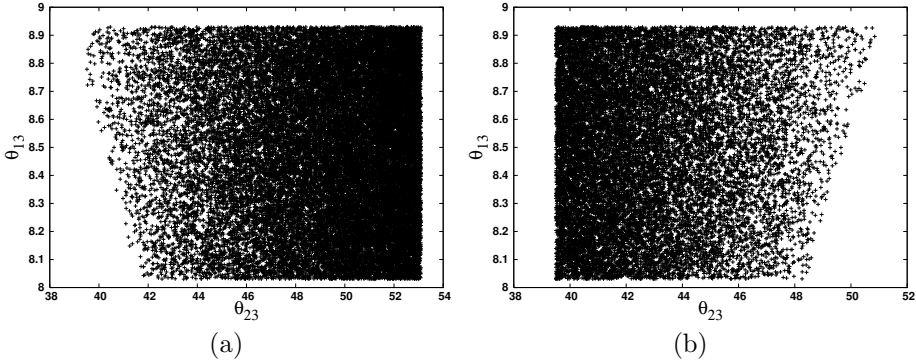


Figure 6: Correlation plots for textures (a) P_2 and (b) P_3 , depicting the permutation symmetry.

Here $\eta \cdot \kappa = \pm 1$ and the upper and lower signs in the above expression refer to cases $\delta = 0^\circ$ and 180° , respectively. For $\delta = 180^\circ$, we find $m_2 < m_1$, which is in contradiction with solar neutrino oscillation data. Using Eqs. (61) and (62), R_ν can be given as

$$R_\nu \approx \beta^2 - \alpha^2 \approx \frac{3}{2} \left(\frac{s_{23}s_{13}}{c_{12}s_{12}c_{23}} \right). \quad (63)$$

For normal mass ordering, taking into account the 3σ experimental range of oscillation parameters, we find, $0.235 \leq R_\nu \leq 0.468$, which excludes the experimental range of R_ν . Similarly, for inverted mass ordering, texture P_4 is found to be ruled out. Since textures P_5 and P_4 are phenomenologically related to each other due to permutation symmetry, therefore texture P_5 also remains inconsistent with latest experimental data at 3σ level.

3.4.2 Texture P_6 with $\text{Tr } M_\nu = 0$

Using Eqs. (28) and (29), we deduce some analytical expressions in leading order of s_{13} term.

$$\alpha \equiv \frac{m_1}{m_3} \approx -\frac{1}{\eta} \sec 2\theta_{12}(1 + c_{12}^2), \quad (64)$$

$$\beta \equiv \frac{m_2}{m_3} \approx \frac{1}{\kappa} \sec 2\theta_{12}(1 + s_{12}^2), \quad (65)$$

where $\eta, \kappa = \pm 1$. From Eqs. (64) and (65), we find that $m_2 < m_1$, therefore, texture P_6 with $\text{Tr } M_\nu = 0$ is ruled out for both normal as well as inverted mass ordering at 3σ CL.

The neutrino mass matrices for two allowed textures viz. P_2 and P_3 with $\text{Tr } M_\nu = 0$ are given below:

$$M_\nu^{P_2} = \begin{pmatrix} c_{11} & c_{12} & c_{13} \\ c_{21} & c_{22} & c_{23} \\ c_{31} & c_{32} & c_{33} \end{pmatrix},$$

where

$$\begin{aligned} c_{11} &= 0.0104 - 0.0211, \\ c_{12} &= ((-0.0402) - (-0.0154)) + i((-0.0252) - 0.0253), \\ c_{13} &= (0.0178 - 0.0374) + i((-0.0329) - 0.0324), \\ c_{21} &= ((-0.0402) - (-0.0154)) - i((-0.0252) - 0.0253), \\ c_{22} &= 0.0, \\ c_{23} &= (0.00506 - 0.00926) + i((-0.00651) - 0.00638), \\ c_{31} &= (0.0178 - 0.0374) - i((-0.0329) - 0.0324), \\ c_{32} &= (0.00506 - 0.00926) - i((-0.00651) - 0.00638), \\ c_{33} &= (-0.0211) - (-0.0104), \end{aligned}$$

and

$$M_\nu^{P_3} = \begin{pmatrix} d_{11} & d_{12} & d_{13} \\ d_{21} & d_{22} & d_{23} \\ d_{31} & d_{32} & d_{33} \end{pmatrix},$$

where

$$\begin{aligned}
d_{11} &= 0.0103 - 0.0193, \\
d_{12} &= (0.0196 - 0.0369) + i(-0.0291 - 0.0297), \\
d_{13} &= ((-0.0397) - (-0.0183)) + i((-0.0293) - 0.0297), \\
d_{21} &= (0.0196 - 0.0369) - i((-0.0291) - 0.0297), \\
d_{22} &= (-0.0193) - (-0.0104), \\
d_{23} &= (0.00544 - 0.00912) + i((-0.00594) - 0.00570), \\
d_{31} &= ((-0.0397) - (-0.0183)) - i((-0.0293) - 0.0297), \\
d_{32} &= (0.00544 - 0.00912) - i((-0.00594) - 0.00570), \\
d_{33} &= 0.0.
\end{aligned}$$

From above matrices, we observe that the elements of mass matrices for textures P_2 and P_3 are approximately similar to mass matrix elements for texture one zero with $\text{Det } M_\nu=0$ condition. For the sake of comparison, the range of δ has been provided for both the conditions [Table 7].

4 Summary and conclusions

To summarize our analysis, we have studied the implication of $\text{Det } M_\nu=0$ or $\text{Tr } M_\nu=0$ conditions, on texture one zero neutrino mass matrices, assuming the Dirac nature of neutrinos. The six viable textures have been broadly classified into two categories viz. CP violating (P_1, P_2, P_3) and CP conserving (P_4, P_5, P_6), respectively. Therefore, CP violation is only possible for $P_{1,2,3}$, and we have $\delta = 0$ or π for the other one-zero textures. In the analysis, all the CP conserving textures are found to be ruled out for both normal as well as inverted mass ordering at 3σ CL, however among the CP violating textures, only P_1 and P_2 are able to survive the data for inverted mass ordering.

In Ref. [40, 42], it is explicitly shown that CP-conserving value $\delta = 0$ (or 2π) is disfavored at 3σ in both NO and IO, while $\delta = \pi$ is also disfavored at 3σ in IO but not in NO (where it is still allowed at 2σ). In addition, a preference for CP violation with $\sin\delta < 0$ is indicated at $< 2\sigma$ CL [37, 39, 40, 42]. These experimental indications are motivating as far as our analysis is concerned, however, a precise determination of δ is important to decide the compatibility of these textures. In the end, the phenomenological results of survived textures have been compared for both the conditions.

To conclude our discussion, we would like to mention that it is very difficult to determine the exact nature of neutrinos whether Dirac or Majorana particle under the current experimental scenario. Therefore the assumption of Dirac neutrino carries some motivation. The only possibility in the near future depends on neutrinoless double beta decay experiments, which would determine the Majorana nature of neutrinos. In addition, the absolute neutrino mass is still not known, therefore

the consideration of vanishing neutrino mass or vanishing sum of neutrino masses can not be ruled out at present. The data collected from the Planck satellite [43] combined with other cosmological data, however put a upper limit on the sum of neutrino masses as $\sum_i m_i < 0.23 \text{ eV}$ at 2σ CL. The future and currently running longbaseline experiments, neutrinoless double beta decay experiments and cosmological observations would check the validity of the present analysis and assumptions.

Acknowledgment

The author would like to thank the Director, National Institute of technology (NIT) Kurukshetra, India for providing necessary facilities to work, and special thanks to Dr. Radha Raman Gautam for the useful discussion during this work.

References

- [1] Particle Data Group, K. Nakamura et al., J. Phys. G 37, 075021 (2010).
- [2] K. Abe et al. [T2K collaboration], Phys. Rev. Lett. 107, 041801 (2011), arXiv: 1106.2822 [hep-ex].
- [3] P. Adamson et al. [MINOS collaboration], Phys. Rev. Lett.107, 181802 (2011), arXiv: 1108.0015 [hep-ex].
- [4] Y. Abe et al., [Double Chooz collaboration], Phys. Rev. Lett.108, 131801 (2012), arXiv: 1112.6353 [hep-ex].
- [5] F. P. An et al., [Daya Bay collaboration], Phys. Rev. Lett.108, 171803 (2012), arXiv: 1203.1669 [hep-ex].
- [6] Soo-Bong Kim, for RENO collaboration, Phys. Rev. Lett.108, 191802 (2012), arXiv: 1204.0626[hep-ex].
- [7] C. I. Low, R. R. Volkas, Phys. Rev. D 68, 033007 (2003), hep-ph/0305243; C. S. Lam Phys. Rev. D 74, 113004 (2006), hep-ph/0611017.
- [8] S. Weinberg, Trans. New York Acad. Sci. 38, 185 (1977); F. Wilczek and A. Zee, Phys. Lett. 70B, 418 (1977); H. Fritzsch, Phys. Lett. 70B, 436 (1977); Phys. Lett. 73B, 317 (1978); Nucl. Phys. B155, 18 (1979).
- [9] H. Fritzsch and Z.Z. Xing, Prog. Part. Nucl. Phys. 45, 1 (2000); Z.Z. Xing, Int. J. Mod. Phys. A 19, 1 (2004); arXiv:hep-ph/0406049.
- [10] Paul H. Frampton, Sheldon L. Glashow and Danny Marfatia, Phys. Lett. B 536, 79 (2002),hep-ph/0201008.

- [11] Zhi-zhong Xing, Phys. Lett. B 530, 159 (2002), hep-ph/0201151; H. Fritzsch, Z. Z. Xing, Phys. Lett. B 517 (2001) 363-368, arXiv: hep-ph/0103242.
- [12] Bipin R. Desai, D. P. Roy and Alexander R. Vaucher, Mod. Phys. Lett. A 18, 1355 (2003), hep-ph/0209035; A. Merle, W. Rodejohann, Phys. Rev. D 73, 073012 (2006), hep-ph/0603111; S. Dev, Sanjeev Kumar, S. Verma and S. Gupta, Nucl. Phys. B 784, 103-117 (2007), hep-ph/0611313; S. Dev, S. Kumar, S. Verma and S. Gupta, Phys. Rev. D 76, 013002 (2007), hep-ph/0612102; M. Randhawa, G. Ahuja, M. Gupta, Phys. Lett. B 643, 175-181 (2006), hep-ph/0607074; G. Ahuja, S. Kumar, M. Randhawa, M. Gupta, S. Dev, Phys. Rev. D 76, 013006 (2007), hep-ph/0703005; S. Kumar, Phys. Rev. D 84, 077301 (2011), arXiv: 1108.2137 [hep-ph]; P. O. Ludl, S. Morisi, E. Peinado, Nucl. Phys. B 857, 411 (2012), arXiv: 1109.3393 [hep-ph]; Manmohan Gupta, Gulshleen Ahuja, Int. J. Mod. Phys. A, 27, 1230033 (2012), arXiv:1302.4823 [hep-ph]; D. Meloni, G. Blankenburg, Nucl. Phys. B 867, 749 (2013), arXiv:1204.2706 [hep-ph]; W. Grimus, P. O. Ludl, J. Phys. G40, 055003 (2013), arXiv:1208.4515 [hep-ph]; S. Sharma, P. Fakay, G. Ahuja and M. Gupta arXiv: 1402.1598 [hep-ph]; P. O. Ludl, W. Grimus, arXiv:1406.3546v1 [hep-ph]; H. Fritzsch, Zhi-zhong Xing, S. Zhou, JHEP 1109, 083 (2011), arXiv: 1108.4534 [hep-ph]; Madan Singh, Gulshleen Ahuja, Manmohan Gupta, Prog. Theor. Exp. Phys. (PTEP) 2016 (12): 123B 08, arXiv: 1603.08083 [hep-ph]; Madan Singh, Adv. High Energy Phys. 2018(2018) 2863184, arXiv: 1803.10735[hep-ph].
- [13] C. Hagedorn and W. Rodejohann, JHEP 0507, 034 (2005).
- [14] X. Liu, S. Zhou, Int. J. Mod. Phys. A 28 (2013) 1350040.
- [15] E. I. Lashin and N. Chamoun, Phys. Rev. D85, 113011 (2012), arXiv: 1108.4010 [hep-ph].
- [16] K. R. Deines, E. Dudas, and T. Gherghetta, Nucl. Phys. B 557, 25 (1999); N. Arkani-Hamed, S. Dimopoulos, G. Dvali, and J. March-Russell, Phys. Rev. D 65, 024032 (2001).
- [17] H. Murayama, Nucl. Phys. Proc. Suppl. 137, 206 (2004).
- [18] S. Abel, A. Dedes and K. Tamvakis, Phys. Rev. D 71, 033003 (2005); H. Davoudiasl, R. Kitano, G. D. Kribs and H. Murayama, hep-ph/0502176.
- [19] G. C. Branco and G. Senjanovic, Phys. Rev. D 18, 1621 (1978); D. Chang and R. N. Mohapatra, Phys. Rev. Lett. 58, 1600 (1987); P. Q. Hung, Phys. Rev. D 59, 113008 (1999); arXiv: hep-ph/0006355.
- [20] M. Fukugita and T. Yanagida, Phys. Lett. B 174, 45 (1986).
- [21] K. Dick et al., Phys. Rev. Lett. 84, 4039 (2000); H. Murayama and A. Pierce, Phys. Rev. Lett. 89, 271601 (2002).

- [22] E. K. Akhmedov, V. A. Rubakov and A. Y. Smirnov, Phys. Rev. Lett. 81, 1359 (1998).
- [23] G. C. Branco, et al., Phys. Lett. B 562 (2003) 265.
- [24] W. Grimus, L. Lavoura, Phys. Rev. D 62 (2000) 093012; T. Asaka, et al., Phys. Rev. D 62 (2000) 123514; R. Kuchimanchi, R. N. Mohapatra, Phys. Rev. D 66 (2002) 051301; P.H. Frampton, S. L. Glashow, T. Yanagida, Phys. Lett. B 548 (2002) 119; T. Endoh, et al., Phys. Rev. Lett. 89 (2002) 231601; M. Raidal, A. Strumia, Phys. Lett. B 553 (2003) 72; B. Dutta, R. N. Mohapatra, hep-ph/0305059.
- [25] Z. Z. Xing, Phys. Rev. D 69, 013006 (2004); W. Rodejohann, M. Tanimoto, A. Watanabe, arXiv : 1201.4936 [hep-ph]; L. Lavoura, W. Rodejohann, A. Watanabe, arXiv :1307.6421[hep-ph].
- [26] H. Murayama and T. Yanagida, Phys. Lett. B 322, 349 (1994) [arXiv: hep-ph/9310297].
- [27] T. Asaka, M. Fujii, K. Hamaguchi and T. Yanagida, Phys. Rev. D 62, 123514 (2000) [arXiv: hep-ph/0008041].
- [28] M. Fujii, K. Hamaguchi and T. Yanagida, Phys. Rev. D 64, 123526 (2001) [arXiv: hep-ph/0104186].
- [29] R. R. Gautam, Madan Singh, M. Gupta Phys. Rev. D, 92 (2015), 013006, arXiv:1506.04868 [hep-ph].
- [30] D. Black, et al., Phys. Rev. D 62 (2000) 073015.
- [31] X. G. He, A. Zee, Phys. Rev. D 68 (2003) 037302, hep-ph/0302201.
- [32] A. Zee, Phys. Lett. B 93 (1980) 389; A. Zee, Phys. Lett. B 95 (1980) 461, Erratum; L. Wolfenstein, Nucl. Phys. B 175 (1980) 93.
- [33] H. A. Alhendi , E. I. Lashin and A. A. Mudlej, Phys. Rev. D 77, 013009, arXiv: 0708.2007 [hep-ph].
- [34] W. Rodejohann, Phys. Lett. B 579 (2004) 127139, arXiv:0308119v1[hep-ph].
- [35] SNO Collaboration, Q.R. Ahmad et al., Phys. Rev. Lett. 89, 011301 (2002); Phys. Rev.Lett. 89, 011302 (2002).
- [36] KamLAND Collaboration, K. Eguchi et al., Phys. Rev. Lett. 90, 021802 (2003).
- [37] I. Esteban, et al., JHEP 01, 087 (2017), arXiv: 1611.01514 [hep-ph].
- [38] P. Adamson et al. (NOvA), Phys. Rev. Lett. 118, 231801 (2017), arXiv:1703.03328 [hep-ex].

- [39] P. F. de Salas, D. V. Forero, C. A. Ternes, M. Tortola, J. W. F. Valle, arXiv:1708.01186 [hep-ph].
- [40] F. Capozzi, E. Lisi, A. Marrone, A. Palazzo, arXiv: 1804.09678 [hep-ph].
- [41] A. Radovic, "Latest Neutrino Oscillation Results from NOvA," seminar at Fermilab (12 January 2018), available at <https://www-nova.fnal.gov>. See also the subsequent NOvA talks, up to March 2018.
- [42] M. Hartz, "T2K Neutrino Oscillation Results with Data up to 2017 Summer," seminar at KEK (4 August 2017), available at <https://www.t2k.org/docs/talk> (talk n. 282 in the list). See also the subsequent T2K talks, up to March 2018.
- [43] P. A. R. Ade et al., [Planck Collaboration], arXiv: 1502.01589 [astro-ph.CO].

Texture	$\frac{m_2}{m_3}$	status
P_1	$-\frac{1}{\kappa} \frac{t_{13}^2}{s_{12}^2}$	unviable
P_2	$-\frac{1}{\kappa} \frac{s_{23}^2 c_{13}^2}{s_{12}^2 s_{23}^2 s_{13}^2 + c_{12}^2 c_{23}^2 - 2s_{12}s_{23}s_{13}c_{12}c_{23}c_\delta}$	unviable
P_3	$-\frac{1}{\kappa} \frac{c_{23}^2 c_{13}^2}{s_{12}^2 c_{23}^2 s_{13}^2 + c_{12}^2 s_{23}^2 + 2s_{12}s_{23}c_{12}c_{23}s_{13}c_\delta}$	unviable
P_4	$-\frac{1}{\kappa} \frac{s_{23}s_{13}}{-s_{12}^2 s_{23}s_{13} \pm s_{12}c_{12}c_{23}}$	unviable
P_5	$-\frac{1}{\kappa} \frac{c_{23}c_{13}s_{13}}{-s_{12}^2 c_{23}c_{13}s_{13} \mp s_{12}c_{12}c_{13}s_{23}}$	unviable
P_6	$-\frac{1}{\kappa} \frac{s_{23}c_{23}c_{13}^2}{(s_{12}^2 s_{13}^2 - c_{12}^2)c_{23}s_{23} + s_{12}c_{12}s_{13}(\pm s_{23}^2 \mp c_{23}^2)}$	unviable

Table 3: The exact expressions of mass ratio $\frac{m_2}{m_3}$ along with the status of all the six one zero textures with $m_1 = 0$ (normal mass ordering) is shown. The upper and lower signs in the above expressions refer to cases $\delta = 0^\circ$ and 180° , respectively.

Texture	$\frac{m_2}{m_1}$	status
P_1	$-\frac{\eta}{\kappa} \frac{1}{t_{12}^2}$	unviable
P_2	$-\frac{\eta}{\kappa} \frac{c_{12}^2 s_{23}^2 s_{13}^2 + s_{12}^2 c_{23}^2 + 2s_{12}s_{23}c_{12}c_{23}s_{13}c_\delta}{s_{12}^2 s_{23}^2 s_{13}^2 + c_{12}^2 c_{23}^2 - 2s_{12}s_{23}c_{12}c_{23}s_{13}c_\delta}$	viable
P_3	$-\frac{\eta}{\kappa} \frac{c_{12}^2 c_{23}^2 s_{13}^2 + s_{12}^2 s_{23}^2 - 2s_{12}s_{23}c_{12}c_{23}s_{13}c_\delta}{s_{12}^2 c_{23}^2 s_{13}^2 + c_{12}^2 s_{23}^2 + 2s_{12}s_{23}c_{12}c_{23}s_{13}c_\delta}$	viable
P_4	$-\frac{\eta}{\kappa} \frac{1}{t_{12}} \cdot \frac{-s_{23}c_{12}s_{13} \mp s_{12}c_{23}}{-s_{23}s_{12}s_{13} \pm c_{12}c_{23}}$	unviable
P_5	$-\frac{\eta}{\kappa} \frac{1}{t_{12}} \cdot \frac{-c_{12}c_{23}s_{13} \pm s_{12}s_{23}}{-s_{12}c_{23}s_{13} \mp c_{12}s_{23}}$	unviable
P_6	$-\frac{\eta}{\kappa} \frac{s_{23}c_{23}(c_{12}^2 s_{13}^2 - s_{12}^2) + s_{12}c_{12}s_{13}(\pm c_{23}^2 \mp s_{23}^2)}{s_{23}c_{23}(s_{12}^2 s_{13}^2 - c_{12}^2) + s_{12}c_{12}s_{13}(\pm s_{23}^2 \mp c_{23}^2)}$	unviable

Table 4: The expressions of mass ratio $\frac{m_2}{m_1}$ alongwith the status of all the six one zero textures with $m_3 = 0$ (inverted mass ordering) is shown. The upper and lower signs in the above expressions refer to cases $\delta = 0^\circ$ and 180° , respectively.

Texture	Analytical expressions for $\frac{m_1}{m_3}$ and $\frac{m_2}{m_3}$	NO	IO
P_1	$\alpha = \frac{1}{\eta} \sec 2\theta_{12}(s_{12}^2 - t_{13}^2)$ $\beta = -\frac{1}{\kappa} \sec 2\theta_{12}(c_{12}^2 - t_{13}^2)$	unviable	unviable
P_2	$\alpha = \frac{1}{\eta} \frac{(s_{12}^2 s_{13}^2 - c_{13}^2) s_{23}^2 + c_{12} c_{23} (c_{12} c_{23} - 2s_{12} s_{23} s_{13} c_{\delta})}{(s_{23}^2 s_{13}^2 - c_{23}^2) c_{2(12)} + s_{2(12)} s_{2(23)} s_{13} c_{\delta}}$ $\beta = \frac{1}{\kappa} \frac{(-c_{12}^2 s_{13}^2 + c_{13}^2) s_{23}^2 - s_{12} c_{23} (s_{12} c_{23} + 2c_{12} s_{23} s_{13} c_{\delta})}{(s_{23}^2 s_{13}^2 - c_{23}^2) c_{2(12)} + s_{2(12)} s_{2(23)} s_{13} c_{\delta}}$	unviable	viable
P_3	$\alpha = \frac{1}{\eta} \frac{(s_{12}^2 s_{13}^2 - c_{13}^2) c_{23}^2 + c_{12} s_{23} (c_{12} s_{23} + 2s_{12} c_{23} s_{13} c_{\delta})}{(c_{23}^2 s_{13}^2 - s_{23}^2) c_{2(12)} - s_{2(12)} s_{2(23)} s_{13} c_{\delta}}$ $\beta = \frac{1}{\kappa} \frac{(-c_{12}^2 s_{13}^2 + c_{13}^2) c_{23}^2 - s_{12} s_{23} (s_{12} s_{23} - 2c_{12} c_{23} s_{13} c_{\delta})}{(c_{23}^2 s_{13}^2 - s_{23}^2) c_{2(12)} - s_{2(12)} s_{2(23)} s_{13} c_{\delta}}$	unviable	viable
P_4	$\alpha = \frac{1}{\eta} \frac{s_{23} s_{13} (1 + s_{12}^2) \mp s_{12} c_{12} c_{23}}{s_{23} s_{13} (c_{12}^2 - s_{12}^2) \pm 2s_{12} c_{12} c_{23}}$ $\beta = -\frac{1}{\kappa} \frac{s_{23} s_{13} (1 + c_{12}^2) \pm s_{12} c_{12} c_{23}}{s_{23} s_{13} (c_{12}^2 - s_{12}^2) \pm 2s_{12} c_{12} c_{23}}$	unviable	unviable
P_5	$\alpha = \frac{1}{\eta} \frac{c_{23} s_{13} (1 + s_{12}^2) \pm s_{12} c_{12} c_{23}}{c_{23} s_{13} (c_{12}^2 - s_{12}^2) \mp 2s_{12} c_{12} s_{23}}$ $\beta = -\frac{1}{\kappa} \frac{c_{23} s_{13} (1 + c_{12}^2) \mp s_{12} c_{12} s_{23}}{c_{23} s_{13} (c_{12}^2 - s_{12}^2) \mp 2s_{12} c_{12} s_{23}}$	unviable	unviable
P_6	$\alpha = \frac{1}{\eta} \frac{s_{23} c_{23} (s_{12}^2 s_{13}^2 - c_{12}^2 - c_{13}^2) + c_{12} s_{12} s_{13} (\pm s_{23}^2 \mp c_{23}^2)}{s_{23} c_{23} (1 + s_{13}^2) c_{2(12)} \mp 2s_{12} c_{12} s_{13}}$ $\beta = \frac{1}{\kappa} \frac{s_{23} c_{23} (-c_{12}^2 s_{13}^2 + s_{12}^2 + c_{13}^2) + c_{12} s_{12} s_{13} (\mp s_{23}^2 \pm c_{23}^2)}{s_{23} c_{23} (1 + s_{13}^2) c_{2(12)} \mp 2s_{12} c_{12} s_{13}}$	unviable	unviable

Table 5: The exact expressions of mass ratios $\alpha \equiv \frac{m_1}{m_3}$ and $\beta \equiv \frac{m_2}{m_3}$ alongwith the status of all the six one zero textures with vanishing trace (i.e. $\text{Tr } M_{\nu} = 0$) is shown. The upper and lower signs in the above expressions refer to the cases $\delta = 0^{\circ}$ and 180° , respectively. The symbols $c_{2(ij)} \equiv \cos 2\theta_{ij}$, $s_{2(ij)} \equiv \sin 2\theta_{ij}$ are defined.

Texture	signs of η and κ	NO	IO
P_1	$\eta = +1, \kappa = +1$	×	×
	$\eta = +1, \kappa = -1$	×	×
	$\eta = -1, \kappa = +1$	×	×
	$\eta = -1, \kappa = -1$	×	×
P_2	$\eta = +1, \kappa = +1$	×	×
	$\eta = +1, \kappa = -1$	×	allowed
	$\eta = -1, \kappa = +1$	×	×
	$\eta = -1, \kappa = -1$	×	×
P_3	$\eta = +1, \kappa = +1$	×	×
	$\eta = +1, \kappa = -1$	×	allowed
	$\eta = -1, \kappa = +1$	×	×
	$\eta = -1, \kappa = -1$	×	×
P_4	$\eta = +1, \kappa = +1$	×	×
	$\eta = +1, \kappa = -1$	×	×
	$\eta = -1, \kappa = +1$	×	×
	$\eta = -1, \kappa = -1$	×	×
P_5	$\eta = +1, \kappa = +1$	×	×
	$\eta = +1, \kappa = -1$	×	×
	$\eta = -1, \kappa = +1$	×	×
	$\eta = -1, \kappa = -1$	×	×
P_6	$\eta = +1, \kappa = +1$	×	×
	$\eta = +1, \kappa = -1$	×	×
	$\eta = -1, \kappa = +1$	×	×
	$\eta = -1, \kappa = -1$	×	×

Table 6: All possibilities of signs of η and κ , which are associated with the expressions of mass ratios $\frac{m_1}{m_3}$ and $\frac{m_2}{m_3}$ alongwith the status of all the six one zero textures with $\text{Det } M_\nu = 0$ or $\text{Tr } M_\nu = 0$ is shown.

Texture	$(M_\nu)_{lm} = 0$ with $\text{Det } M_\nu = 0$	$(M_\nu)_{lm} = 0$ with $\text{Tr } M_\nu = 0$
P_1	×	×
P_2	$\delta = 0^0 - 53^0 \oplus 306^0 - 360^0$ $J_{CP} = -0.0306 - 0.0300$	$\delta = 0^0 - 53^0 \oplus 306^0 - 360^0$ $J_{CP} = -0.0306 - 0.0300$
P_3	$\delta = 130^0 - 230^0$ $J_{CP} = -0.0291 - 0.0285$	$\delta = 128.5^0 - 231.8^0$ $J_{CP} = -0.0291 - 0.0285$
P_4	×	×
P_5	×	×
P_6	×	×

Table 7: Comparison for allowed ranges of Dirac CP-violating phase(δ) and Jarlskog rephrasing invariant parameter(J_{CP}) for all six one-zero textures with $\text{Det } M_\nu = 0$ and $\text{Tr } M_\nu = 0$ respectively, is shown at 3σ level.

